Sensitivity of the DVCS cross section to the Compton form factors in scalar QED [1]

Ben Bakker

Vrije Universiteit, Faculty of Sciences
Department of Physics and Astronomy
Amsterdam, The Netherlands

Light Cone 2015, Frascati, 24 September 2015

[1] This work was done in collaboration with Chueng Ji

Outline

Motivation

Deeply-virtual Compton scattering (DVCS) has been proposed to determine the generalized-parton distributions (GPDs) of hadrons.

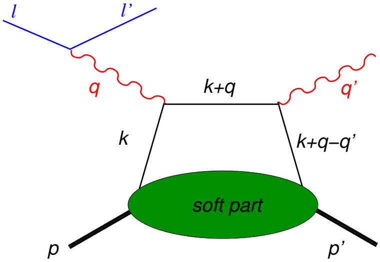

Handbag diagram, including the leptonic part

A hard photon, $q^2 = -Q^2$, with Q much larger than the characteristic hadronic scales, probes the quark content of the hadronic target. The detection of the outgoing, real photon provides information not contained in deep-inelastic scattering (DIS).

It is important to realize that GPDs are not invariant quantities. They are related asymptotically, *i.e.*, for large Q, and for small Mandelstam t to Compton form factors (CFFs).

Even if the experimental data are analysed in terms of these Lorentz-invariant quantities, it is not immediately clear what are the sensitivities of the data to the CFFs.

In a simple case, namely VCS on a scalar target where the minimal number of diagrams that are necessary to maintain EM current conservation are known, the corrections to the tree-level case can be calculated. We have found their scaling with Q^2.

In practice, the VCS amplitude interferes with the Bethe-Heitler amplitude. The latter one does only depend on the EM form factor(s) and thus give by itself no information about the CFFs.

Formalism

We shall concentrate on the DVCS part of the amplitude and even ignore the leptonic part, because it is independent of the CFFs.

In virtual Compton scattering the physical amplitudes can be written as the contraction of a tensor operator with the photon polarization vectors.

It is important to use the most general form of that tensor operator consistent with EM gauge invariance.

We shall briefly discuss two proposals, one by **Tarrach**[2], and the other by **Metz**[3], and compare the two.

[2]M. Perrottet, Lett. Nuovo Cim. **7**, 915 (1973);
R. Tarrach, Nuovo Cim. **28 A**, 409 (1975)

[3]A. Metz, *Virtuelle Comptonstreuung und die Polarisierbarkeiten des Nukleons* (in German), PhD thesis, Universität mainz, 1997.

Tensor Formulation

We write the physical amplitudes as contractions of a tensor with the polarization vectors of the photons:

$$A(h', h) = \epsilon^*(q'; h')_\mu T^{\mu\nu} \epsilon(q; h)_\nu.$$

The tensor $T^{\mu\nu}$ must be transverse, i.e.,

$$q'_\mu T^{\mu\nu} = 0, \quad T^{\mu\nu} q_\nu = 0.$$

The tensor is written in terms of scalars (CFFs) and basis tensors.

In the case we study, namely DVCS on a scalar hadron, to find the number of independent tensor structures we first identify the independent momenta. From four-momentum conservation it follows that out of the 4 external momenta one may choose 3 independent ones.

We keep q and q', to simplify a check of the transversity of the tensor. For the remaining one we choose the sum of the hadronic momenta, $\bar{P} = p' + p$. Our basis is $k_1 = \bar{P}$, $k_2 = q'$, $k_3 = q$.

The most general second-rank tensor expressed in terms of our basis is then:

$$T^{\mu\nu} = \mathcal{T}_0 \; g^{\mu\nu} + \sum_{i,j} \mathcal{T}_{ij} \; k_i{}^{\mu} k_j{}^{\nu}.$$

By contracting $T^{\mu\nu}$ with q'_μ and q_ν, which must give the result 0 for the physical tensor, one can determine the number of independent scalars $\mathcal{T}$.

As there are 10 $\mathcal{T}$s and the number of independent contractions is 5, there are 5 CFFs in the **effective** tensor.

As the 5 independent tensor structures can be chosen in an infinite number of ways, we look for a synthetic way to construct the effective tensor.

Note the difference with the case of a spin-1/2 target, where the γ-matrices can be included in the basis for the tensor. This leads to a tensor with **18** independent parts.

Following Tarrach, we find it useful to construct the tensor $T^{\mu\nu}$ by applying a two-sided projector $\tilde{g}^{\mu\nu}(q,q')$ to the most general second rank tensor expressed in terms of our basis:

$$T^{\mu\nu} = \tilde{g}^{\mu m}\, t_{mn}\, \tilde{g}^{n\nu}, \quad t_{mn} = t_0\, g_{mn} + \sum_{i,j} t_{ij}\; k_{i\,m} k_{j\,n}.$$

The two-sided projector $\tilde{g}(q,q')$ is defined as follows:

$$\tilde{g}^{\mu\nu}(q,q') = g^{\mu\nu} - \frac{q^\mu q'^\nu}{q\cdot q'}.$$

This projector has the properties

$$\tilde{g}^{\mu m}\, g_{mn}\, \tilde{g}^{n\nu} = \tilde{g}^{\mu\nu}, \quad q'_\mu\, \tilde{g}^{\mu\nu} = 0, \quad \tilde{g}^{\mu\nu} q_\nu = 0.$$

The application of $\tilde{g}^{\mu m}$ and $\tilde{g}^{n\nu}$ removes the parts of t_{mn} that contain the left factor q_m or the right factor q'_n.

We define the reduced momenta, $(k = \bar{P},\ q',\ q)$:

$$\tilde{k}_{\mathrm{L}}^{\mu} = \tilde{g}^{\mu m} k_m, \quad \tilde{k}_{\mathrm{R}}^{\nu} = k_n \tilde{g}^{n\nu}$$

and find for unrestricted kinematics the followoing result for $T^{\mu\nu}$

$$T^{\mu\nu} = \mathcal{H}_0\ \tilde{g}^{\mu\nu} + \mathcal{H}_1\ \tilde{P}_{\mathrm{L}}^{\mu} \tilde{P}_{\mathrm{R}}^{\nu} + \mathcal{H}_2\ \tilde{P}_{\mathrm{L}}^{\mu} \tilde{q}_{\mathrm{R}}^{\nu} + \mathcal{H}_3\ \tilde{q}_{\mathrm{L}}^{\prime\mu} \tilde{P}_{\mathrm{R}}^{\nu} + \mathcal{H}_4\ \tilde{q}_{\mathrm{L}}^{\prime\mu} \tilde{q}_{\mathrm{R}}^{\nu}.$$

Contracting the tensor with $\epsilon_{\mu}^{*}(q')$ and $\epsilon_{\nu}(q)$ we find that all **5** pieces of the tensor contribute, if $q'^2 \neq 0$ and $q^2 \neq 0$.

The number of independent tensor structures is equal to the number of independent physical matrix elements consistent with parity conservation: $A(-h', -h) = (-1)^{h'-h} A(h', h),\ h', h = \pm 1, 0,$

$$A(1,1),\ A(1,0),\ A(1,-1),\ A(0,1),\ \text{and}\ A(0,0).$$

If either of the photons is real, some pieces of the tensor do not contribute to the physical amplitudes: the tensor is reduced to an **effective** tensor.

For instance, consider the case where one of the photons is real, say $q'^2 = 0$, then the number of independent physical amplitudes reduces to 3, say $A(1,1)$, $A(1,0)$, and $A(1,-1)$.

The vector $\tilde{q}'_L$ reduces to q' which is orthogonal to $\epsilon(q')$ and thus the CFFs $\mathcal{H}_3$ and $\mathcal{H}_4$ do not contribute, reducing the full tensor $T^{\mu\nu}$ to an effective one with only 3 independent pieces.

Finally, if both photons are real, the number of active CFFs reduces to 2, which equals the number of independent physical amplitudes $A(1,1)$ and $A(1,-1)$. The effective tensor has in this case the same form as the tree-level tensor.

Thus, the number of CFFs in the **effective** tensor equals the number of independent physical matrix elements.

Metz's approach

The method using the projectors introduces a kinematical singularity at $q' \cdot q = 0$. In Tarrach's paper a method is described to remove these kinematic poles. Here we give the final result of that algorithm as obtained in the thesis of Metz. His CFFs in the scalar case are denoted as $\mathcal{B}_1$, $\mathcal{B}_2$, $\mathcal{B}_3$, $\mathcal{B}_4$, and $\mathcal{B}_{19}$. They are implicitly given in terms of the elementary tensor by the following equations:

$$
\begin{aligned}
M^{\mu\nu} &= \mathcal{B}_1 M_1^{\mu\nu} + \mathcal{B}_2 M_2^{\mu\nu} + \mathcal{B}_3 M_3^{\mu\nu} + B_4 M_4^{\mu\nu} + B_{19} M_{19}^{\mu\nu}, \\
M_1^{\mu\nu} &= -q' \cdot q\, g^{\mu\nu} + q^\mu q'^\nu, \\
M_2^{\mu\nu} &= -(\bar{P} \cdot q)^2 g^{\mu\nu} - q' \cdot q\, \bar{P}^\mu \bar{P}^\nu + \bar{P} \cdot q\, (\bar{P}^\mu q'^\nu + q^\mu \bar{P}^\nu), \\
M_3^{\mu\nu} &= q'^2 q^2 g^{\mu\nu} + q' \cdot q\, q'^\mu q^\nu - q^2 q'^\mu q'^\nu - q'^2 q^\mu q^\nu, \\
M_4^{\mu\nu} &= \bar{P} \cdot q\, (q'^2 + q^2)\, g^{\mu\nu} - \bar{P} \cdot q\, (q'^\mu q'^\nu + q^\mu q^\nu) \\
&\quad -q^2 \bar{P}^\mu q'^\nu - q'^2 q^\mu \bar{P}^\nu + q' \cdot q\, (\bar{P}^\mu q^\nu + q'^\mu \bar{P}^\nu), \\
M_{19}^{\mu\nu} &= (\bar{P} \cdot q)^2 q'^\mu q^\nu + q'^2 q^2 \bar{P}^\mu \bar{P}^\nu - \bar{P} \cdot q\, q^2 q'^\mu \bar{P}^\nu - \bar{P} \cdot q\, q'^2 \bar{P}^\mu q^\nu.
\end{aligned}
$$

Metz's five basis tensors are also transverse to q'_μ and q_ν. One can easily check that the following expansions of the M_j in terms of Tarrach's transverse momenta holds:

$$\begin{aligned}
M_1^{\mu\nu} &= -q' \cdot q\, \tilde{g}^{\mu\nu}, \\
M_2^{\mu\nu} &= -(\bar{P} \cdot q)^2\, \tilde{g}^{\mu\nu} - q' \cdot q\, \tilde{P}_\mathrm{L}^\mu \tilde{P}_\mathrm{R}^\nu, \\
M_3^{\mu\nu} &= {q'}^2 q^2\, \tilde{g}^{\mu\nu} + q' \cdot q\, \tilde{q}_\mathrm{L}'^\mu \tilde{q}_\mathrm{R}^\nu, \\
M_4^{\mu\nu} &= \bar{P} \cdot q\, ({q'}^2 + q^2)\, \tilde{g}^{\mu\nu} + q' \cdot q\, (\tilde{P}_\mathrm{L}^\mu \tilde{q}_\mathrm{R}^\nu + \tilde{q}_\mathrm{L}'^\mu \tilde{P}_\mathrm{R}^\nu), \\
M_{19}^{\mu\nu} &= {q'}^2 q^2\, \tilde{P}_\mathrm{L}^\mu \tilde{P}_\mathrm{R}^\nu - \bar{P} \cdot q\, {q'}^2\, \tilde{P}_\mathrm{L}^\mu \tilde{q}_\mathrm{R}^\nu - \bar{P} \cdot q\, q^2\, \tilde{q}_\mathrm{L}'^\mu \tilde{P}_\mathrm{R}^\nu + (\bar{P} \cdot q)^2\, \tilde{q}_\mathrm{L}'^\mu \tilde{q}_\mathrm{R}^\nu.
\end{aligned}$$

To check the transversity of $M^{\mu\nu}$ one needs to use the identity

$$\bar{P} \cdot q = \bar{P} \cdot q'.$$

The relations between the CFFs $\mathcal{H}_i$ and the CFFs $\mathcal{B}_j$ is found by identifying $M^{\mu\nu}$ and $T^{\mu\nu}$. The results are

$$\begin{aligned}
\mathcal{H}_0 &= -q'\cdot q\,\mathcal{B}_1 - (\bar{P}\cdot q)^2\,\mathcal{B}_2 + {q'}^2 q^2\,\mathcal{B}_3 + \bar{P}\cdot q\,({q'}^2 + q^2)\,\mathcal{B}_4,\\
\mathcal{H}_1 &= -q'\cdot q\,\mathcal{B}_2 + q^2{q'}^2\,\mathcal{B}_{19},\\
\mathcal{H}_2 &= q'\cdot q\,\mathcal{B}_4 - \bar{P}\cdot q\,{q'}^2\mathcal{B}_{19},\\
\mathcal{H}_3 &= q'\cdot q\,\mathcal{B}_4 - \bar{P}\cdot q\,q^2\mathcal{B}_{19},\\
\mathcal{H}_4 &= q'\cdot q\,\mathcal{B}_3 + (\bar{P}\cdot q)^2\,\mathcal{B}_{19}.
\end{aligned}$$

If ${q'}^2 = 0$, which is the case we treat here, the independent CFFs are $\mathcal{B}_{1,2}$, and $\mathcal{B}_4$, which agrees with the number of independent amplitudes.

Tree-level DVCS

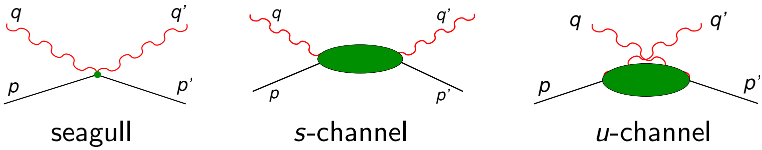

The tree-level DVCS amplitude corresponds in Tarrach formulation to the CFFs

$$\mathcal{H}_0^{\text{tree}} = -2,\ \mathcal{H}_1^{\text{tree}} = \frac{1}{s-M^2} + \frac{1}{u-M^2},\ \mathcal{H}_3^{\text{tree}} = 0,$$

and in Metz formulation

$$\mathcal{B}_1^{\text{tree}} = \frac{1}{s-M^2} + \frac{1}{u-M^2},\ \mathcal{B}_2^{\text{tree}} = -\frac{2}{(s-M^2)(u-M^2)},\ \mathcal{B}_4^{\text{tree}} = 0,$$

$s = (p+q)^2,\ u = (p-q')^2$, M is the target hadron's mass.

Amplitudes

Here, we shall not use any dynamical model for the CFFs, but rather use the tree-level CFFs in Metz's formulation to study the sensitivities of the cross sections for the CFFs. In this formulation the whole interval $0 \leq \theta \leq \pi$ can be explored.

As we do not include the Bethe-Heitler amplitudes, we shall consider the VCS amplitudes only.

In a simple model where the internal structure of the target is included at one-loop level, one finds that the corrections to the tree-level CFFs scale as $\log Q^2/Q^2$. Therefore, as a **working hypothesis**, we assume that for an estimate of the sensitivities of the cross section it is not necessary to use a realistic model.

It is known[4] that to second order in g the following diagrams must be included to guarantee EM gauge invariance:

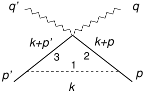

T_{sg}

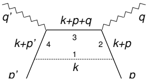

T_{st}

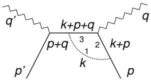

U_{st}

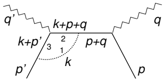

V_{st}

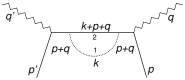

W_{st}

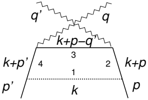

T_{ut}

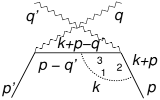

U_{ut}

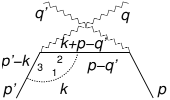

V_{ut}

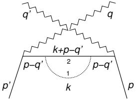

W_{ut}

[4] C.-R. Ji and BLGB, Int. J. Mod. Phys. E **22**, 1330002 (2013)

When the integrals determining the amplitude corresponding to these diagrams are done, one finds that the corrections at one-loop level scale as

$$\frac{1}{Q^n}\log(A+BQ^2),$$

where the functions A and B depend on the Mandelstam variables and the Feynman parameters. The power n is 2 for $\mathcal{H}_0$ and 4 for $\mathcal{H}_{1,2}$ The imaginary parts scale as $1/Q^n$

We shall not consider this model in the present work. Instead we use the tree-level CFFs in Metz's formulation and consider variation by $\pm 10\%$ for $\mathcal{B}_1$ and $\mathcal{B}_2$ to study the sensitivity of the cross section to them. Furthermore, we add a third CFF, namely $\mathcal{B}_4$ for which we take 0 (the tree-level value) and $\pm 0.1\ \mathcal{B}_2$.

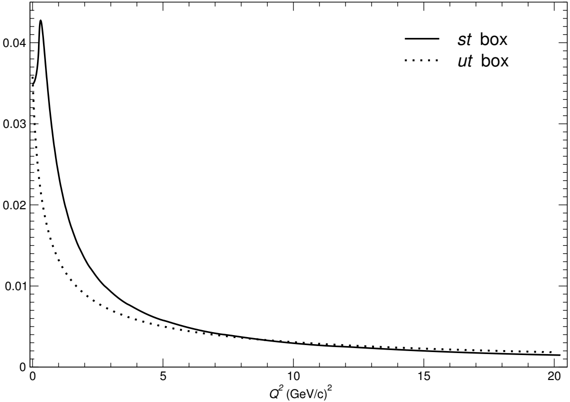

Real parts of the two handbag diagrams: T_{st} and T_{ut}. Amplitude in arbitrary units.

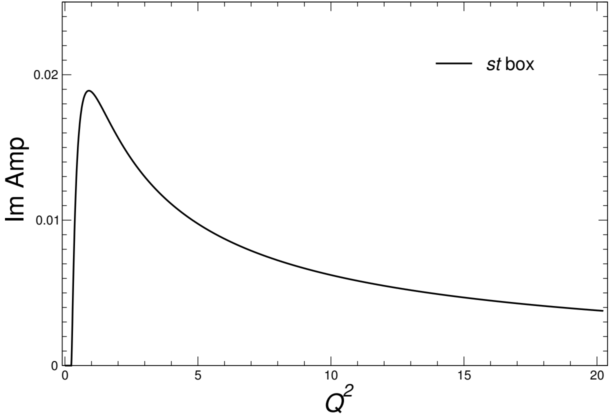

Imaginary part of the s-channel handbag T_{st}. Amplitude in arbitrary units.

Kinematics

In the hadronic CMF the momenta are defined as

$$\begin{aligned}
p^{\mu} &= (E_{\rm C}, -q_{\rm C}\sin\theta_{\rm C}, 0, -q_{\rm C}\cos\theta_{\rm C}),\\
q^{\mu} &= (q^0_{\rm C}, q_{\rm C}\sin\theta_{\rm C}, 0, q_{\rm C}\cos\theta_{\rm C}),\\
p'^{\mu} &= (E'_{\rm C}, -q'_{\rm C}\sin\theta'_{\rm C}, 0, -q'_{\rm C}\cos\theta'_{\rm C}),\\
q'^{\mu} &= (q'_{\rm C}, q'_{\rm C}\sin\theta'_{\rm C}, 0, q'_{\rm C}\cos\theta'_{\rm C}).
\end{aligned}$$

with

$$\begin{aligned}
q_{\rm C} &= \frac{\sqrt{(s-M^2-Q^2)^2+4sQ^2}}{2\sqrt{s}}, \quad E_{\rm C} = \frac{s+M^2+Q^2}{2\sqrt{s}},\\
q^0_{\rm C} &= \frac{s-M^2-Q^2}{2\sqrt{s}},\\
q'_{\rm C} &= \frac{s-M^2}{2\sqrt{s}}, \quad E'_{\rm C} = \frac{s+M^2}{2\sqrt{s}}.
\end{aligned}$$

Superficially, the momenta scale as Q^2, but we can use the Bjorken variable $x_{\rm Bj}$ to relate the Mandelstam variable s to the mass M and Q^2.

Using the definition of the Bjorken variable: $x_{\mathrm{Bj}} = Q^2/(2p \cdot q)$, we find

$$x_{\mathrm{Bj}} = \frac{Q^2}{s + Q^2 - M^2} \leftrightarrow s = M^2 + \frac{1 - x_{\mathrm{Bj}}}{x_{\mathrm{Bj}}} Q^2.$$

Thus s is of order Q^2, which shows that in the CMF all non-vanishing momentum components are of order Q.

It is common practice in the treatment of DVCS, to rotate the coordinate system such that the z-axis is along the three-momentum of the virtual photon. Then $\theta_C = 0$. The quantity $\theta := \theta'_{\mathrm{C}} - \theta_{\mathrm{C}}$, the scattering angle in the CMF, then coincides with θ'_{C}.

Polarization vectors

To calculate the amplitudes, we need the polarization vectors. The polarization vectors of the incoming virtual photon in the CMF are

$$\begin{aligned} \epsilon^\mu(q,\pm 1) &= \frac{1}{\sqrt{2}}(0,\mp\cos\theta_\mathrm{C}, i, \pm\sin\theta_\mathrm{C}) \\ \epsilon^\mu(q,0) &= \frac{1}{\sqrt{-Q^2}}(q_\mathrm{C}, q^0_\mathrm{C}\sin\theta_\mathrm{C}, 0, q^0_\mathrm{C}\cos\theta_\mathrm{C}) \end{aligned}$$

The ones for the final state are obtained by replacing θ_C by θ'_C and q^0 and q_C by q'_C, and dropping the one with helicity 0.

Numerical calculations

We calculate the tree-level amplitudes for two realistic kinematical situations, given in a document written by **Julie Roche** and co-workers. We take the kinematics for the lowest value of the virtuality of the photon considered there, namely $Q^2 = 1.9\ \text{GeV}^2$, and the largest, $Q^2 = 9\ \text{GeV}^2$.

Then we use the Metz tensor to calculate the amplitudes using the tree-level CFFs and vary their numerical values in a range of $\pm 10\%$.

Finally, we calculate the model-dependent part of the DVCS cross section, *i.e.*, the sum of the squared amplitudes over the spin components. Because we consider a scalar target, the only spin degrees of freedom are the helicities of the virtual and the real photon.

Because of parity conservation,

$$A(-h', -h) = (-1)^{h'-h} A(h', h), h', h = \pm 1, 0,$$

we find no polarization:

$$\sum_h |A(1, h)|^2 - |A(-1, h)|^2 = 0.$$

Measurements of the Electron-Helicity Dependent Cross Sections of Deeply Virtual Compton Scattering with CEBAF at 12 GeV

Julie Roche*

Rutgers, The State University of New Jersey, Piscataway, New Jersey 08854; and Thomas Jefferson National Accelerator Facility, Newport News, Virginia 23606†

Charles E. Hyde-Wright‡* and G. Gavalian, M. Amarian, S. Bültmann, G.E. Dodge, H. Juengst, J. Lachniet, A. Radyushkin, P.E. Ulmer, L.B. Weinstein

Old Dominion University, Norfolk VA

Bernard Michel* and J. Ball, P.-Y. Bertin §, M. Brossard, R. De Masi, M. Garçon, F.-X. Girod, M. Guidal, M. Mac Cormick, M. Mazouz, S. Niccolai, B. Pire, S. Procureur, F. Sabatié, E. Voutier, S. Wallon

LPC (Clermont) / LPSC (Grenoble) / IPNO & LPT (Orsay) / CPhT-Polytechnique (Palaiseau) / SPhN (Saclay) CEA/DSM/DAPNIA & CNRS/IN2P3, France

Carlos Muñoz Camacho*

Los Alamos National Laboratory, Los Alamos NM, 87545

Table III: Detailed DVCS Kinematics. The first line is from E00-110, and is included for comparison purposes. The angle θ_q is the central angle of the virtual photon direction $q = (k - k')$.

Q^2 (GeV^2)	$x_{\rm Bj}$	k (GeV)	k' (GeV)	θ_e ($^\circ$)	θ_q ($^\circ$)	$q'(0^\circ)$ (GeV)	W^2 (GeV^2)
1.90	0.36	5.75	2.94	19.3	18.1	2.73	4.2
3.00	0.36	6.60	2.15	26.5	11.7	4.35	6.2
4.00	0.36	8.80	2.88	22.9	10.3	5.83	8.0
4.55	0.36	11.00	4.26	17.9	10.8	6.65	9.0
3.10	0.50	6.60	3.20	22.5	18.5	3.11	4.1
4.80	0.50	8.80	3.68	22.2	14.5	4.91	5.7
6.30	0.50	11.00	4.29	21.1	12.4	6.50	7.2
7.20	0.50	11.00	3.32	25.6	10.2	7.46	8.1
5.10	0.60	8.80	4.27	21.2	17.8	4.18	4.3
6.00	0.60	8.80	3.47	25.6	14.1	4.97	4.9
7.70	0.60	11.00	4.16	23.6	13.1	6.47	6.0
9.00	0.60	11.00	3.00	30.2	10.2	7.62	6.9

- All of the constraints prevent us from kinematics for $x_{\rm Bj} \leq 0.2$.
- Kinematics at $x_{\rm Bj} = 0.7$ are allowed at $k = 8.8$ and 11 GeV. At this time, it is very

We want to know in what kinematical region the greatest sensitivities of the **pseudo cross section**

$$\sum_{h' h} |A(h', h)|^2$$

occurs. Therefore we need to explore for a given x_{Bj} and Q^2 the whole kinematical domain as parametrized by $0 \leq \theta \leq \pi$.

We start with plots of the θ-dependence of the CFFs $\mathcal{B}_1$ and $\mathcal{B}_2$.

$$\mathcal{B}_1^{\text{tree}} = \frac{1}{s - M^2} + \frac{1}{u - M^2}, \; \mathcal{B}_2^{\text{tree}} = -\frac{2}{(s - M^2)(u - M^2)}.$$

The quantity s is independent of θ, so u carries this dependence. Both s and u behave like $1/Q^2$, which explains the scale difference between the plots.

Finally, we compare the case $M = 0.938$ GeV (proton) with the case $M = 3.7273$ GeV (^{4}He). We start with plots of the CFFs.

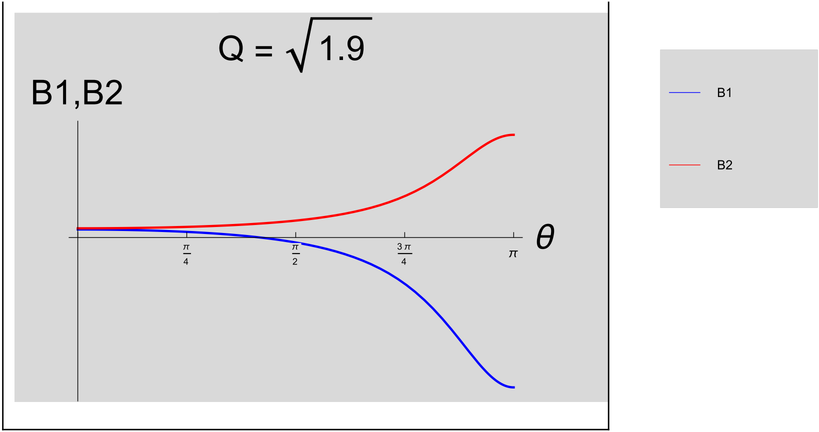

Compton form factors B1 (blue) and B2 (red).
$Q^2 = 1.9\ (\mathrm{GeV}/c)^2$, M $= 0.938\ \mathrm{GeV}/c^2$

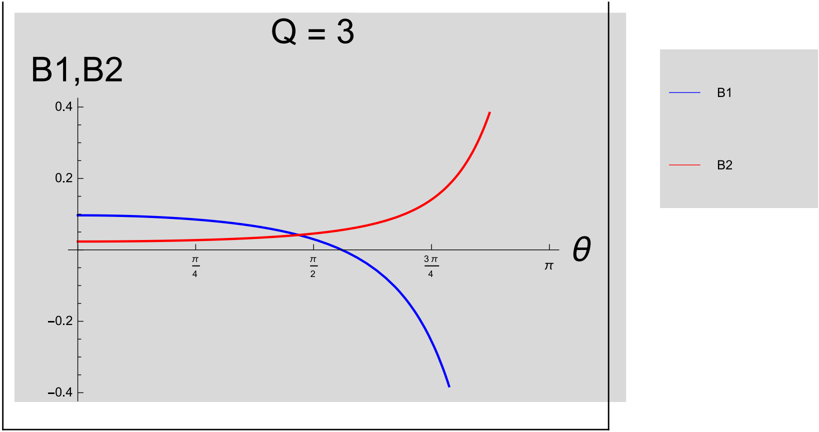

Compton form factors B1 (blue) and B2 (red).
$Q^2 = 9\ (\mathrm{GeV}/c)^2$, $\mathrm{M} = 0.938\ \mathrm{GeV}/c^2$

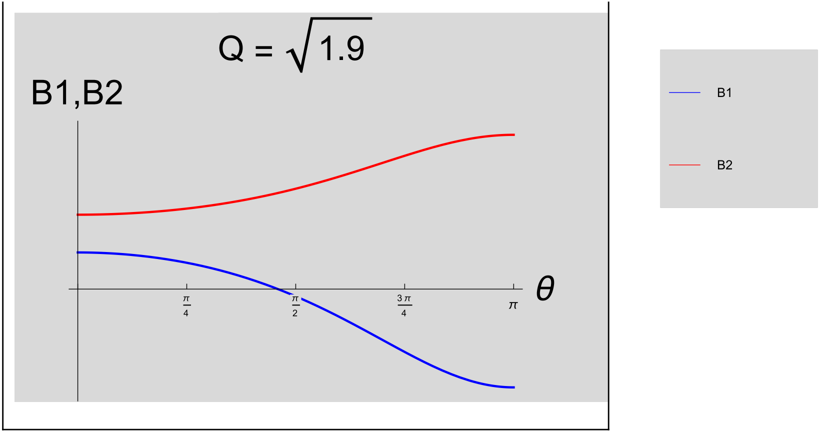

Compton form factors B1 (blue) and B2 (red).
$Q^2 = 1.9\ (\mathrm{GeV}/c)^2$, $\mathrm{M} = 3.7273\ \mathrm{GeV}/c^2$

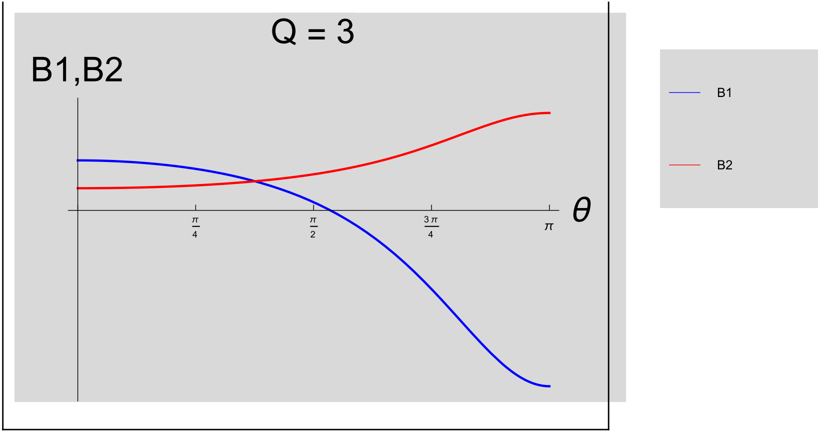

Compton form factors B1 (blue) and B2 (red).
$Q^2 = 9\ (\text{GeV}/c)^2$, M $= 3.7273\ \text{GeV}/c^2$

The next figures show the tree-level Compton amplitudes as a function of θ. At tree-level there exists an additional symmetry

$$A(1,1) + A(1,-1) = 2.$$

The amplitudes $A(\pm 1, 0)$ are purely imaginary at tree level; therefore we plot $A(1,0)/i$ (red curve).

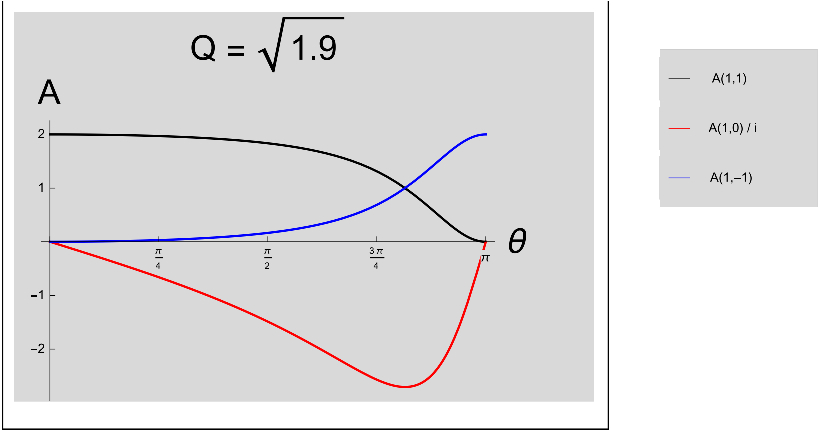

Amplitudes for $Q^2 = 1.9$ $(\mathrm{GeV}/c)^2$, $\mathrm{M} = 0.938$ GeV/c^2

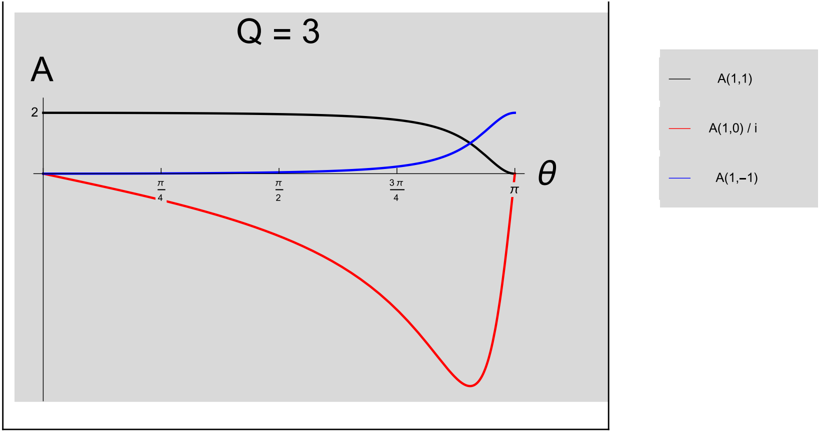

Amplitudes for $Q^2 = 9\ (\mathrm{GeV}/c)^2$, $\mathrm{M} = 0.938\ \mathrm{GeV}/c^2$

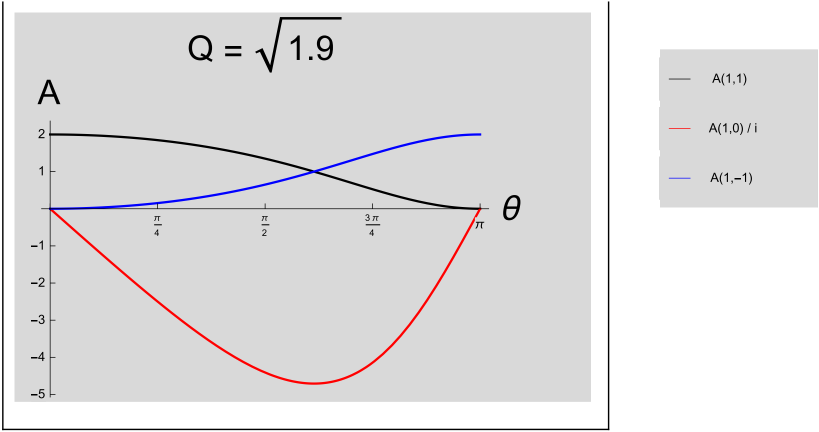

Amplitudes for $Q^2 = 1.9\ (\mathrm{GeV}/c)^2$, $\mathrm{M} = 3.7273\ \mathrm{GeV}/c^2$

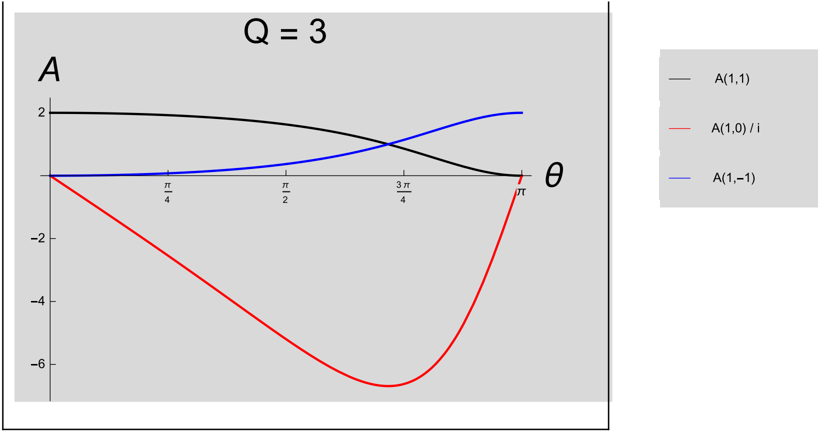

Amplitudes for $Q^2 = 9\ (\mathrm{GeV}/c)^2$, $\mathrm{M} = 3.7273\ \mathrm{GeV}/c^2$

The absolute values of the squared amplitudes are more interesting, because they occur in the cross section.

Notice that the amplitudes $A(\pm 1, 0)$ dominate, at least at large values of θ, which corresponds to **the target recoiling in the forward direction**.

This dominance is less prominent for the larger target mass.

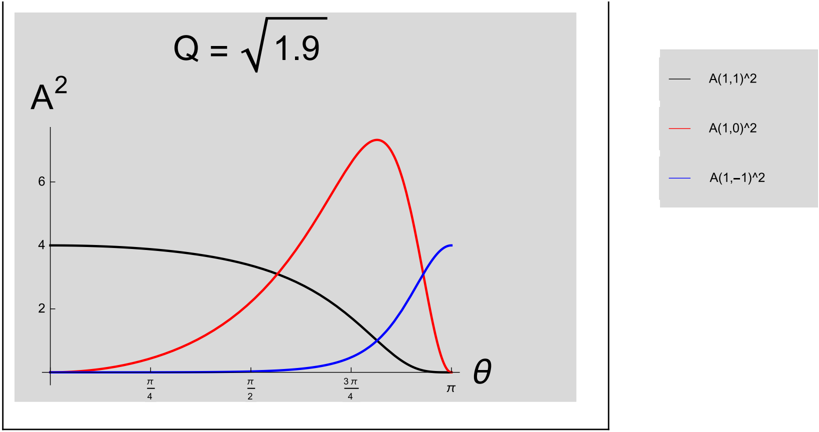

Squared amplitudes for $Q^2 = 1.9\ (\mathrm{GeV}/c)^2$, $\mathrm{M} = 0.938\ \mathrm{GeV}/c^2$

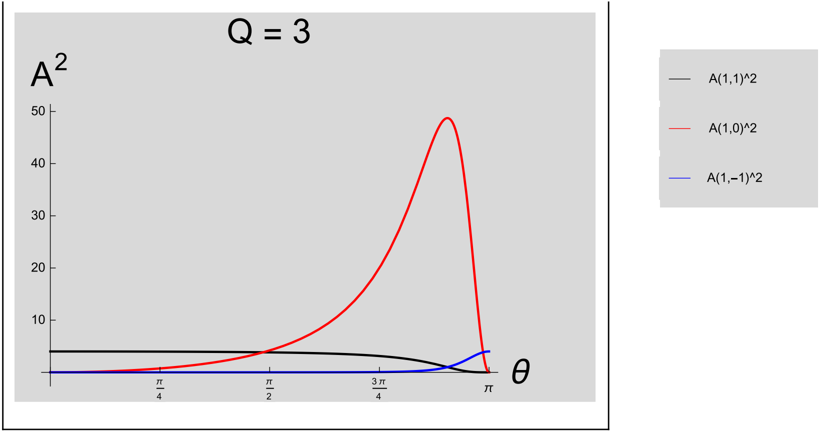

Squared amplitudes for $Q^2 = 9\ (\mathrm{GeV}/c)^2$, $\mathrm{M} = 0.938\ \mathrm{GeV}/c^2$

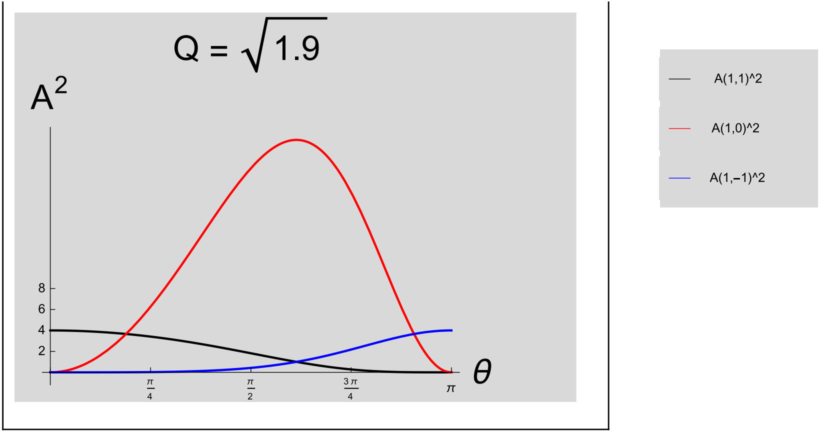

Squared Amplitudes for $Q^2 = 1.9\ (\mathrm{GeV}/c)^2$, $\mathrm{M} = 3.7273\ \mathrm{GeV}/c^2$

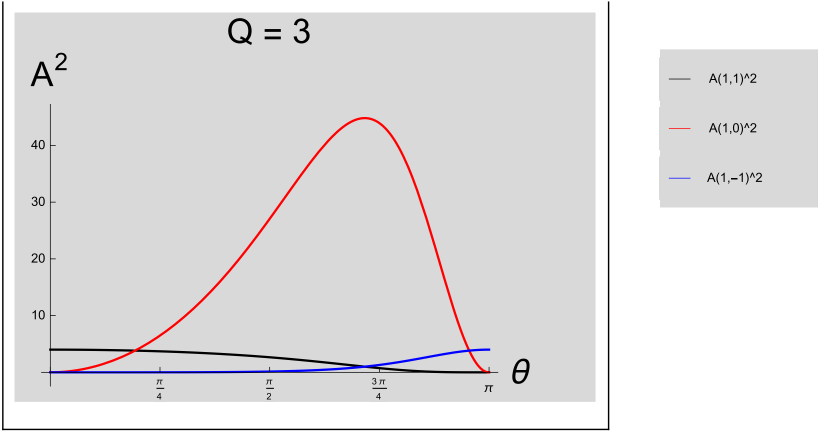

Squared amplitudes for $Q^2 = 9\ (\mathrm{GeV}/c)^2$, $\mathrm{M} = 3.7273\ \mathrm{GeV}/c^2$

The variation of the amplitudes when $\mathcal{B}_1$ is varied by $\pm 10\%$ show that for small target mass and small Q^2 the variations are smaller than for larger target mass and larger Q^2.

The non-flip amplitude $A(1, 1)$ is the least sensitive one, the double flip amplitude $A(1, -1)$ is most sensitive, while $A(1, 0)$, though dominant, varies moderately.

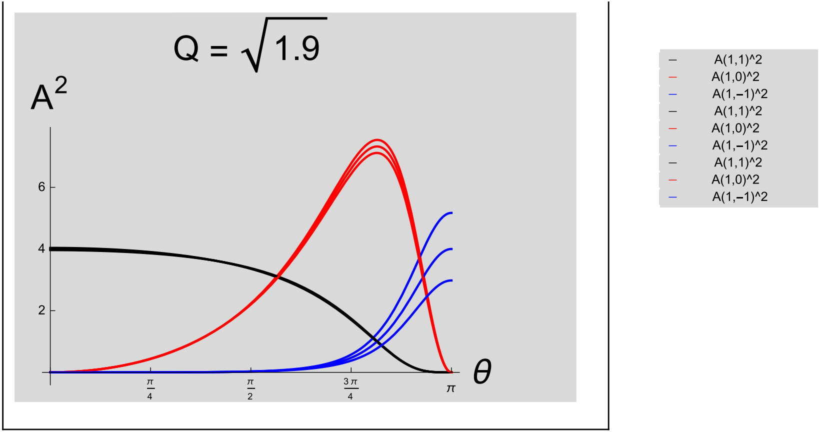

Squared amplitudes for $Q^2 = 1.9\ (\mathrm{GeV}/c)^2$, $\mathrm{M} = 0.938\mathrm{GeV}/c^2$.

The CFF $\mathcal{B}_1$ is varied by $\pm 10\%$

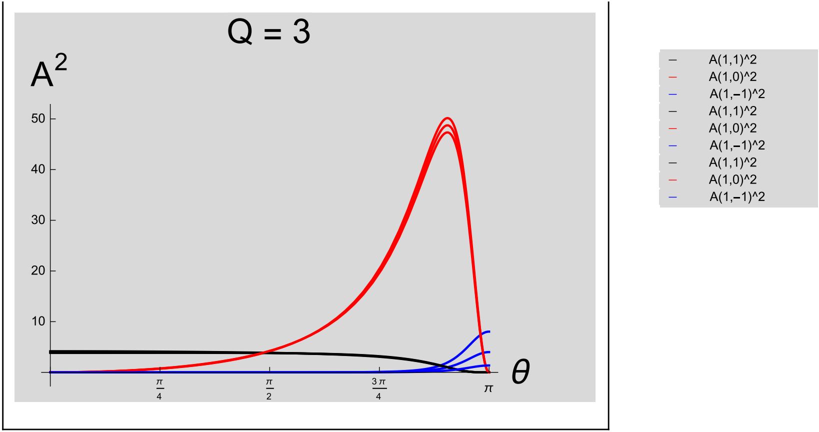

Squared amplitudes for $Q^2 = 9\ (\text{GeV}/c)^2$, $\text{M} = 0.938\ \text{GeV}/c^2$.

The CFF $\mathcal{B}_1$ is varied by $\pm 10\%$

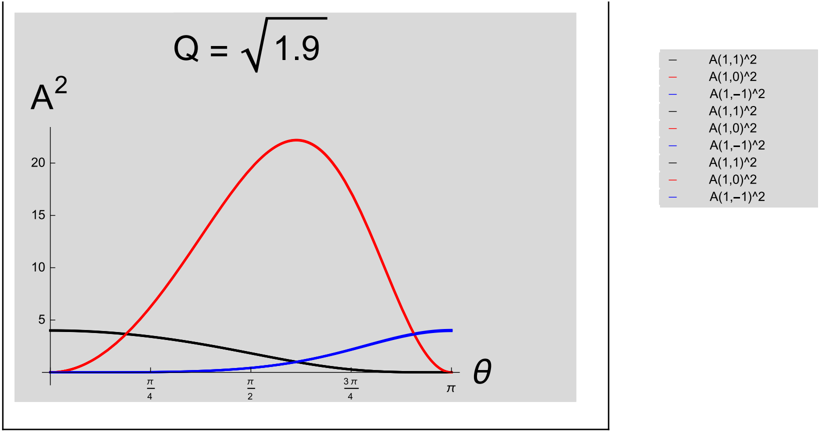

Squared amplitudes for $Q^2 = 1.9\ (\mathrm{GeV}/c)^2$, M $= 3.7273\ \mathrm{GeV}/c^2$.

The CFF $\mathcal{B}_1$ is varied by $\pm 10\%$

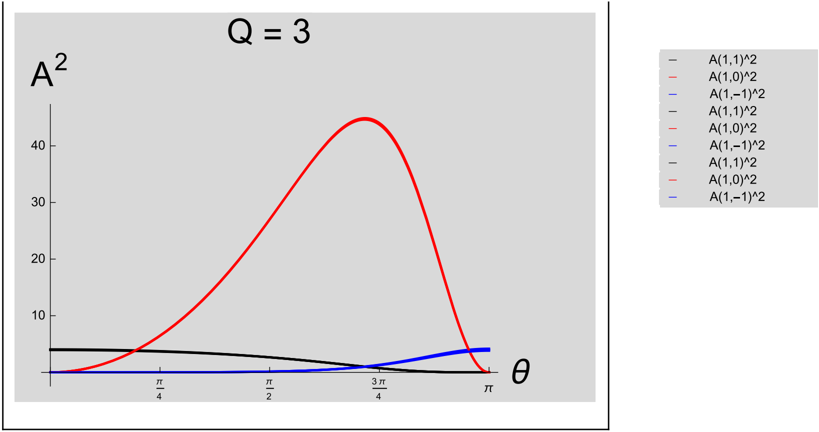

Squared amplitudes for $Q^2 = 9\ (\mathrm{GeV}/c)^2$, $\mathrm{M} = 3.7273\ \mathrm{GeV}/c^2$.

The CFF $\mathcal{B}_1$ is varied by $\pm 10\%$

The variations of the amplitudes when $\mathcal{B}_2$ is varied by $\pm 10\%$ show again that for small target mass and small Q^2 the variations are smaller than for larger target mass and larger Q^2.

However, the variations for all amplitudes are much larger that the ones induced by variation of $\mathcal{B}_1$.

The non-flip amplitude $A(1,1)$ is the least sensitive one, the double flip amplitude $A(1,-1)$ is most sensitive, while $A(1,0)$, though dominant, varies moderately.

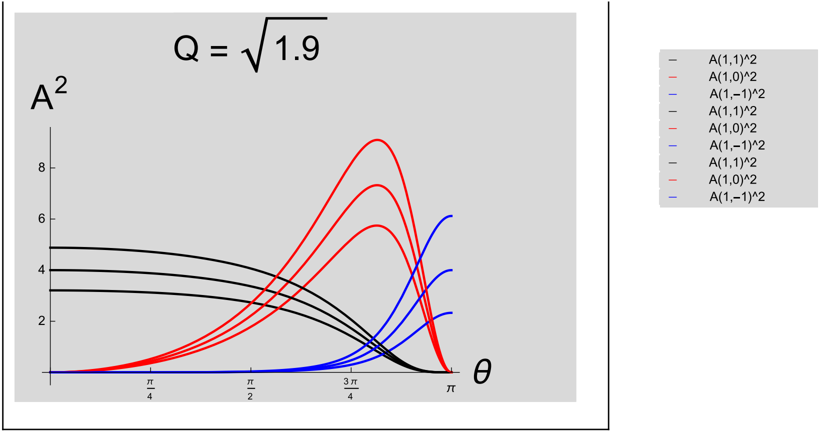

Squared amplitudes for $Q^2 = 1.9\ (\mathrm{GeV}/c)^2$, $\mathrm{M} = 0.938\mathrm{GeV}/c^2$.

The CFF $\mathcal{B}_2$ is varied by $\pm 10\%$

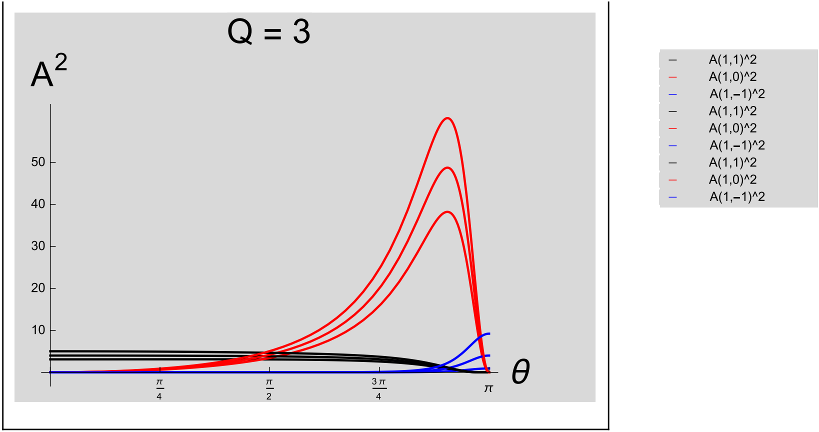

Squared amplitudes for $Q^2 = 9\ (\text{GeV}/c)^2$, $\text{M} = 0.938\ \text{GeV}/c^2$.

The CFF $\mathcal{B}_2$ is varied by $\pm 10\%$

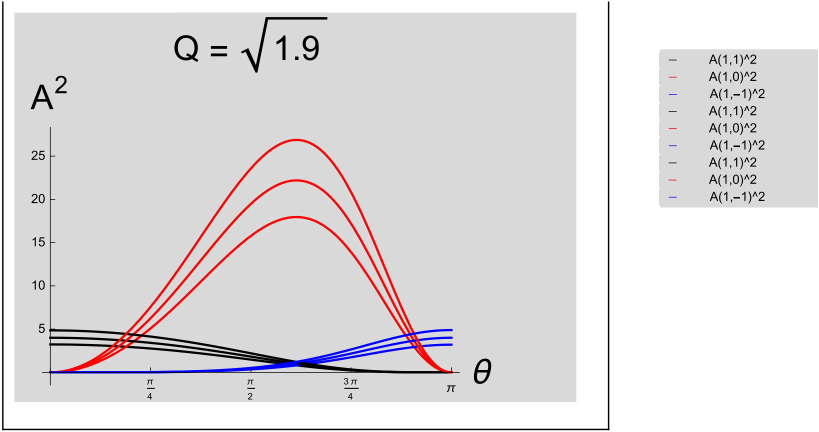

Squared amplitudes for $Q^2 = 1.9\ (\mathrm{GeV}/c)^2$, $\mathrm{M} = 3.7273\ \mathrm{GeV}/c^2$.
The CFF $\mathcal{B}_2$ is varied by $\pm 10\%$

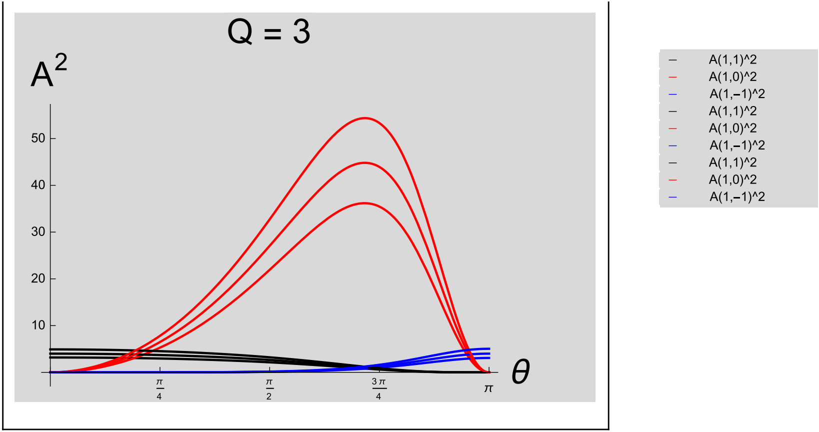

Squared amplitudes for $Q^2 = 9\ (\mathrm{GeV}/c)^2$, $\mathrm{M} = 3.7273\ \mathrm{GeV}/c^2$.

The CFF $\mathcal{B}_2$ is varied by $\pm 10\%$

The variation of the amplitudes when $\mathcal{B}_3$ is varied by $\pm 10\%$ show again that for large target mass M and small Q^2 the variations are smaller than for smaller target mass and larger Q^2.

This dependence on the target mass is much stronger than for the variations induced by $\mathcal{B}_2$.

Again, the non-flip amplitude $A(1,1)$ is the least sensitive one, the double flip amplitude $A(1,-1)$ is most sensitive, while $A(1,0$, though dominant, varies moderately.

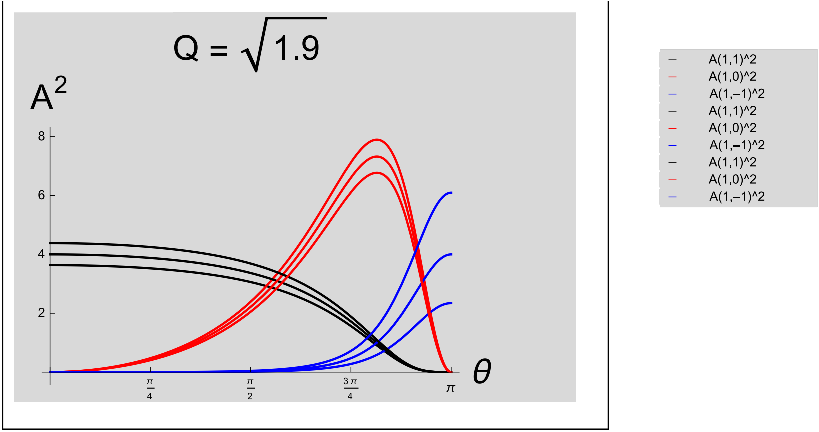

Squared amplitudes for $Q^2 = 1.9$ $(\mathrm{GeV}/c)^2$, $\mathrm{M} = 0.938\mathrm{GeV}/c^2$.
The CFF $\mathcal{B}_3$ is varied by $\pm 10\%$ of $\mathcal{B}_2$

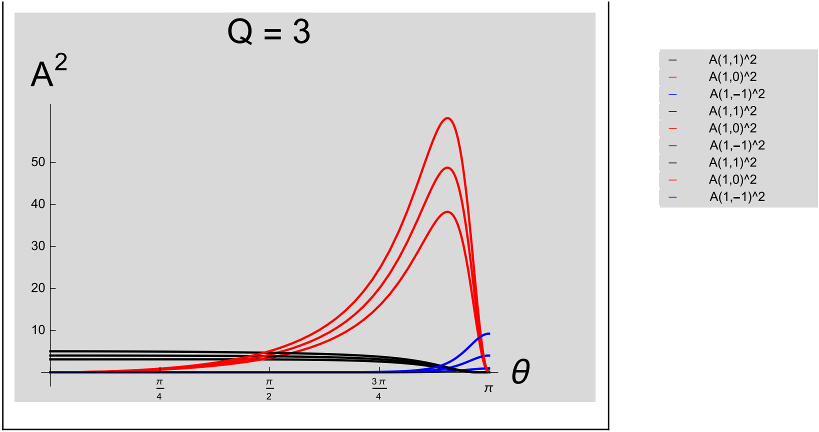

Squared amplitudes for $Q^2 = 9\ (\mathrm{GeV}/c)^2$, $\mathrm{M} = 0.938\ \mathrm{GeV}/c^2$.

The CFF $\mathcal{B}_3$ is varied by $\pm 10\%$ of $\mathcal{B}_2$

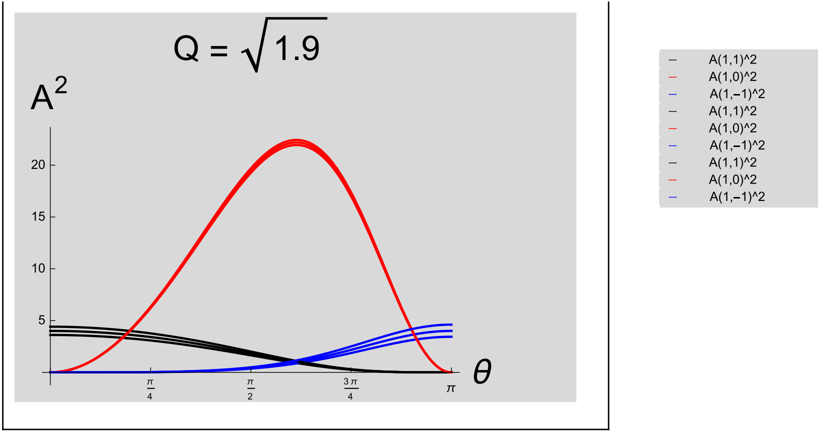

Squared amplitudes for $Q^2 = 1.9\ (\mathrm{GeV}/c)^2$, $\mathrm{M} = 3.7273\ \mathrm{GeV}/c^2$.
The CFF $\mathcal{B}_3$ is varied by $\pm 10\%$ of $\mathcal{B}_2$

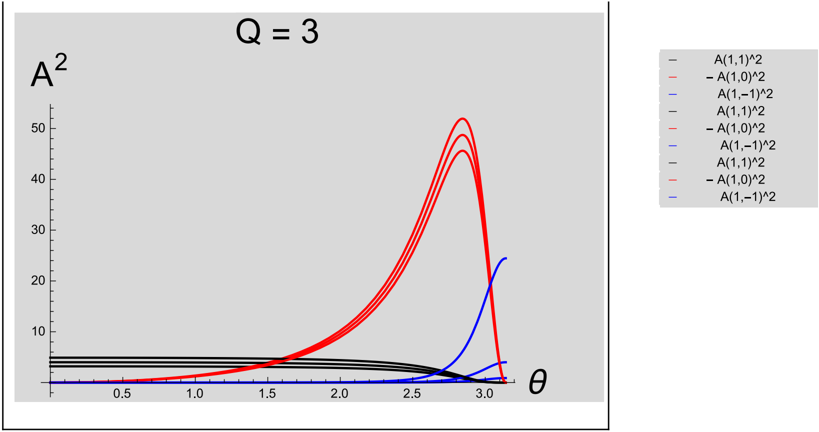

Squared amplitudes for $Q^2 = 9\ (\mathrm{GeV}/c)^2$, $\mathrm{M} = 3.7273\ \mathrm{GeV}/c^2$.
The CFF $\mathcal{B}_3$ is varied by $\pm 10\%$ of $\mathcal{B}_2$

Finally, we show the variations of the pseudo-cross section $\sum |A|^2$.

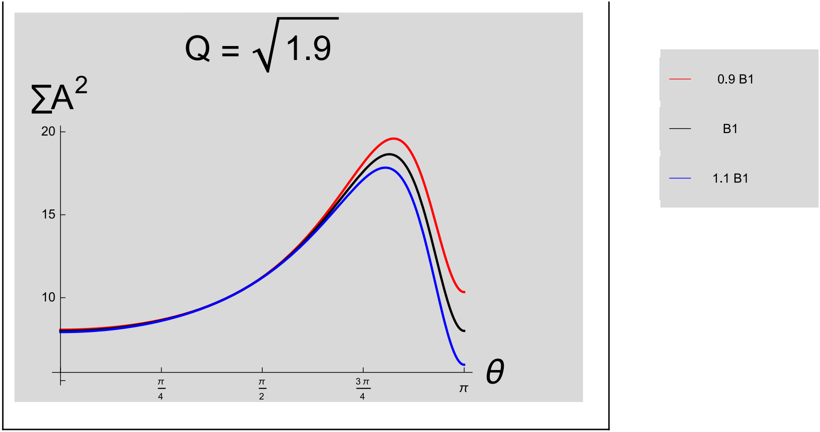

Sum of squared amplitudes for $Q^2 = 1.9\ (\mathrm{GeV}/c)^2$, $\mathrm{M} = 0.938\mathrm{GeV}/c^2$.

The CFF $\mathcal{B}_1$ is varied by $\pm 10\%$

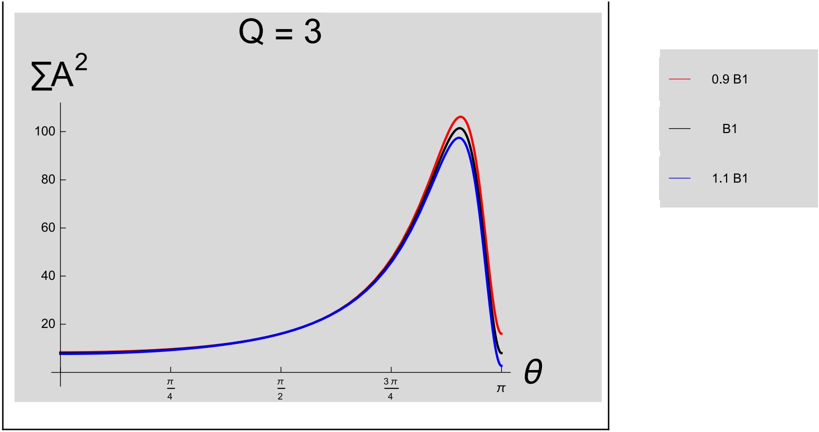

Sum of squared amplitudes for $Q^2 = 9\ (\mathrm{GeV}/c)^2$, $\mathrm{M} = 0.938\ \mathrm{GeV}/c^2$.
The CFF $\mathcal{B}_1$ is varied by $\pm 10\%$

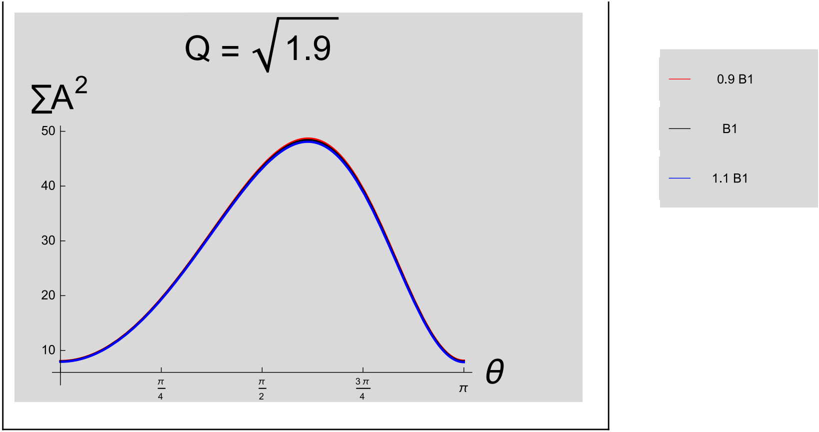

Sum of squared amplitudes for $Q^2 = 1.9\ (\mathrm{GeV}/c)^2$, $\mathrm{M} = 3.7273\ \mathrm{GeV}/c^2$.
The CFF $\mathcal{B}_1$ is varied by $\pm 10\%$

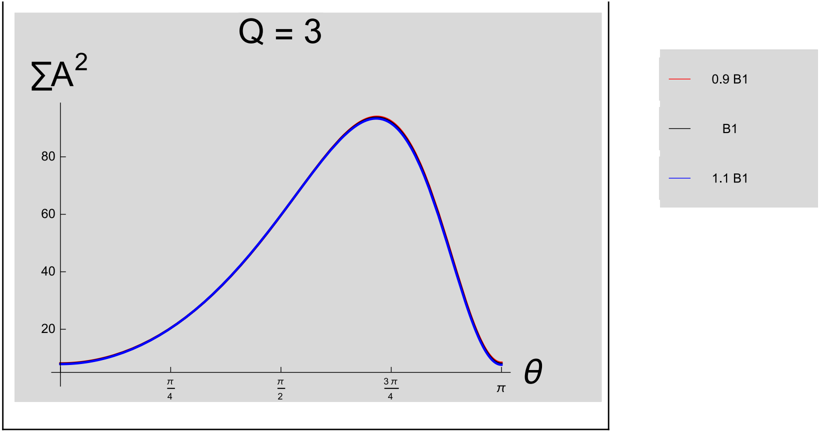

Sum of quared amplitudes for $Q^2 = 9\ (\mathrm{GeV}/c)^2$, $\mathrm{M} = 3.7273\ \mathrm{GeV}/c^2$.

The CFF $\mathcal{B}_1$ is varied by $\pm 10\%$

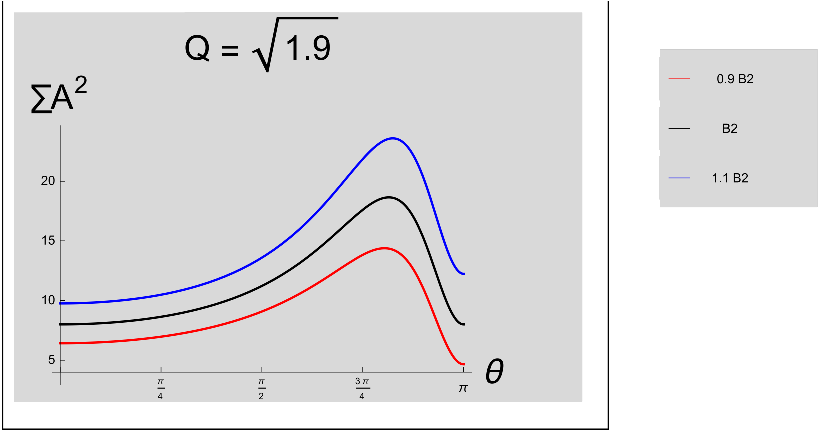

Sum of squared amplitudes for $Q^2 = 1.9\ (\mathrm{GeV}/c)^2$, $\mathrm{M} = 0.938\mathrm{GeV}/c^2$.

The CFF $\mathcal{B}_2$ is varied by $\pm 10\%$

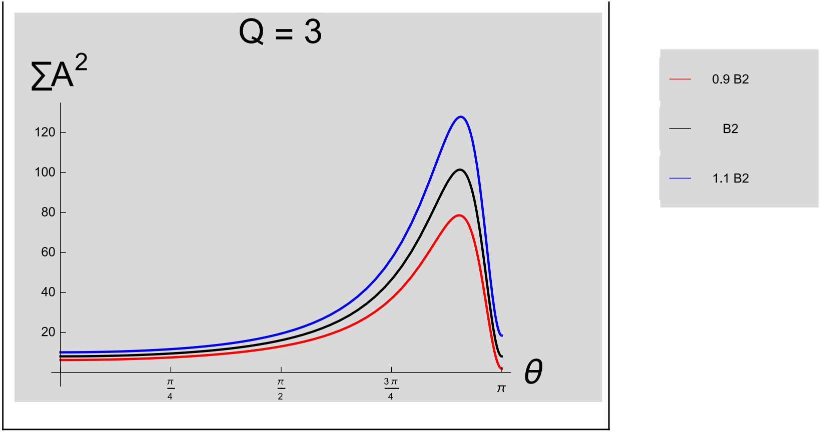

Sum of squared amplitudes for $Q^2 = 9$ $(\text{GeV}/c)^2$, M $= 0.938$ GeV$/c^2$.
The CFF $\mathcal{B}_2$ is varied by $\pm 10\%$

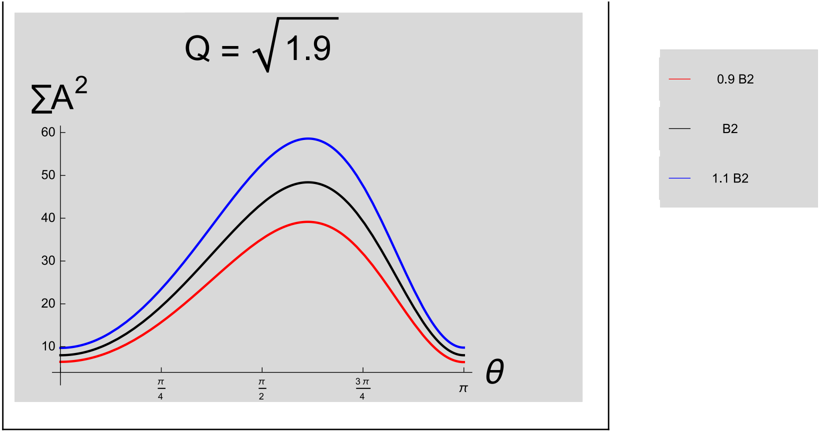

Sum of squared amplitudes for $Q^2 = 1.9$ (GeV/c)^2, M = 3.7273 GeV/c^2.
The CFF $\mathcal{B}_2$ is varied by $\pm 10\%$

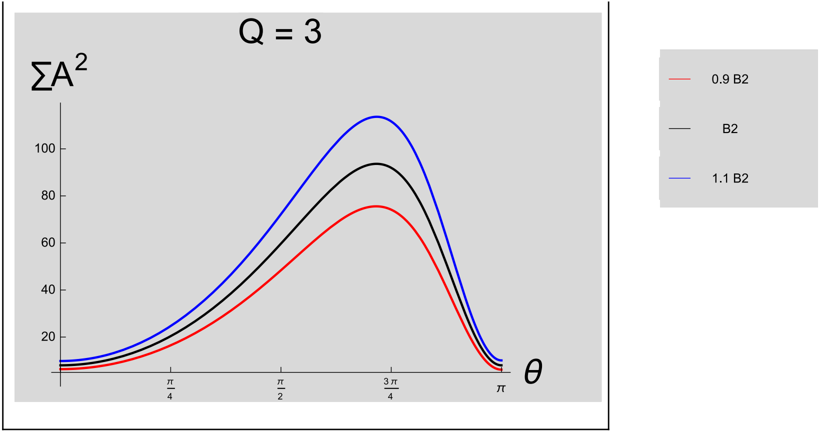

Sum of squared amplitudes for $Q^2 = 9\ (\mathrm{GeV}/c)^2$, $\mathrm{M} = 3.7273\ \mathrm{GeV}/c^2$.

The CFF $\mathcal{B}_2$ is varied by $\pm 10\%$

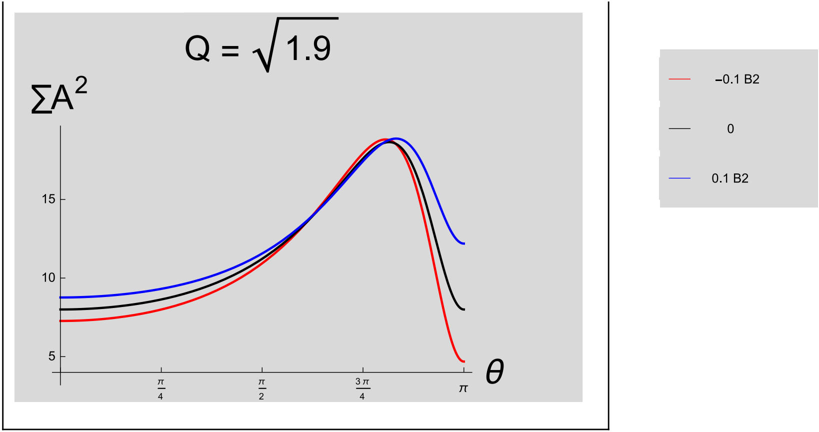

Sum of squared amplitudes for $Q^2 = 1.9$ $(\mathrm{GeV}/c)^2$, M $= 0.938\mathrm{GeV}/c^2$.
The CFF $\mathcal{B}_3$ is varied by $\pm 10\%$ of $\mathcal{B}_2$

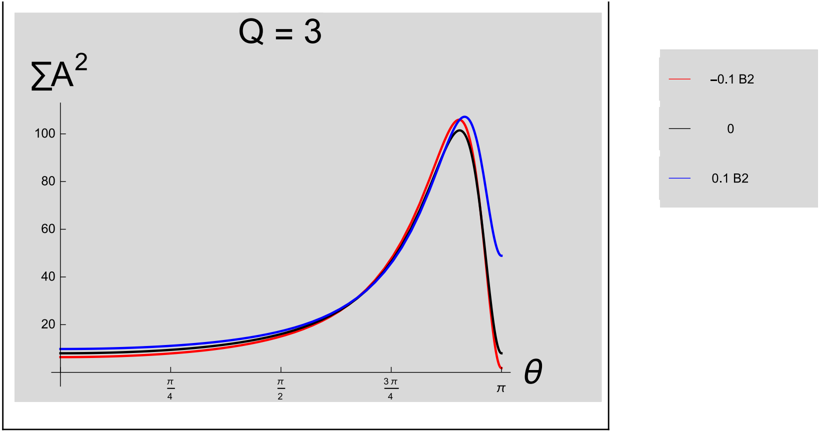

Sum of squared amplitudes for $Q^2 = 9\ (\mathrm{GeV}/c)^2$, $\mathrm{M} = 0.938\ \mathrm{GeV}/c^2$.

The CFF $\mathcal{B}_3$ is varied by $\pm 10\%$ of $\mathcal{B}_2$

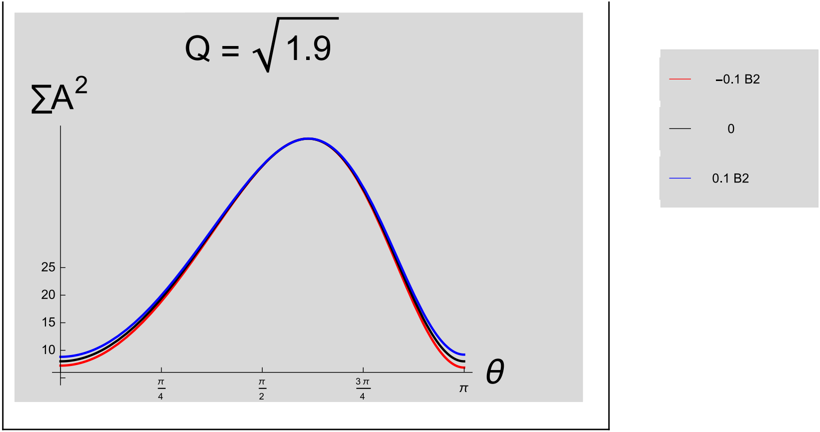

Sum of squared amplitudes for $Q^2 = 1.9$ (GeV/c)^2, M $= 3.7273$ GeV/c^2.
The CFF $\mathcal{B}_3$ is varied by $\pm 10\%$ of $\mathcal{B}_2$

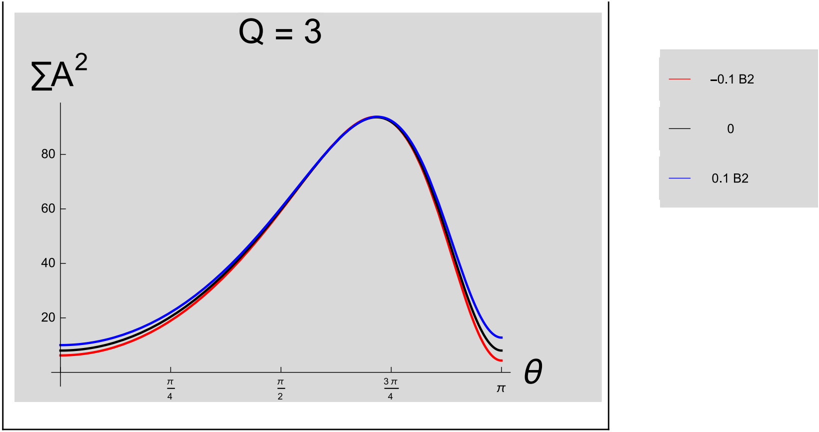

Sum of squared amplitudes for $Q^2 = 9\ (\mathrm{GeV}/c)^2$, M $= 3.7273\ \mathrm{GeV}/c^2$.

The CFF $\mathcal{B}_3$ is varied by $\pm 10\%$ of $\mathcal{B}_2$

Summary and conclusions

1. In the comparatively simple case of DVCS on a scalar target, it is not clear that one can disentangle the differential cross section to determine **all three CFFs**.
2. Only the interference with the Bethe-Heitler may give additional information on the CFFs.
3. The amplitudes $A(\pm i, 0)$ are dominant. In the forward hemisphere where the recoiled target moves forward, these amplitudes are most sensitive to $\mathcal{B}_2$.
4. The basis used by Metz and co-workers can be related linearly to our basis.
5. Using a non-singular basis like Metz's is essential to the analysis of the differential cross section data.